Thermochimica Acta, 237 (1994) 325–332
Elsevier Science B.V., Amsterdam
SSDI 0040-6031(94)01689-E

The kinetics of the thermal reactions of nickel(II) complexes containing *dl*-2,3-butanediamine in a solid phase

Yoshio Masuda [a,*], Noriko Suto [b], Yoshio Ito [b] and Yoshinori Ihara [c]

[a] *Department of Chemistry, College of General Education, Niigata University, Niigata 950-21, Japan*
[b] *Department of Chemistry, Faculty of Science, Niigata University, Niigata 950-21, Japan*
[c] *Laboratory of Chemistry, Faculty of Education, Kanazawa University, Kanazawa 920, Japan*

(Received 9 August 1993; accepted 4 January 1994)

Abstract

The nickel(II) complexes $[Ni(H_2O)_2(dl\text{-bn})_2]X_2$, where (*dl*-bn) is *dl*-2,3-butanediamine and X is Cl^- or Br^-, lose their coordinated water to form square-planar complexes at temperatures ranging from 70 to 90°C. The dehydration is accompanied by thermochromism from violet to yellow. In addition, the dehydrated complexes are thermally isomerized from a square-planar to an octahedral structure by anation of the counter ions, Cl^- or Br^-, in the solid phase at around 180–190°C. The isomerization was also accompanied by distinct thermochromism from yellow to bluish violet.

The kinetics of these dehydrations and isomerizations are studied by means of differential scanning calorimetry (DSC).

The dehydrations of these complexes are considered to follow Avrami–Erofe'ev-type kinetics, and the activation energies for the dehydrations of the chloride and bromide complexes are 80.1 and 87.5 kJ mol^{-1} respectively.

The isomerizations of these complexes are also considered to follow Avrami–Erofe'ev-type kinetics. The activation energies for the isomerizations of the chloride and bromide complexes are 405.4 and 223.8 kJ mol^{-1} respectively.

INTRODUCTION

The coordination structures of various octahedral diaqua-bisbutanediamine-nickel(II) complexes and the products of their thermal reactions have been studied [1–6]. It is known that the bis(N- or C-substituted ethylenediamine) complexes of nickel(II) have either an octahedral or a square-planar structure, depending on the ligand, and that mutual isomerization occurs between these structures [6]. Such isomerizations which include octahedral → square planar → octahedral structural changes, are accompanied by unusual thermochromic changes: violet → yellow → violet.

---

* Corresponding author.

While it is interesting to study the mechanism of the thermal isomerization occurring in a solid phase, such studies have hardly ever been undertaken [7]. Thermal analyses are effective methods for investigating such isomerizations.

In this study, the dehydrations and isomerizations of $[Ni(H_2O)_2(dl\text{-}bn)_2]X_2$ (X is Cl^- or Br^-) were analyzed kinetically using differential scanning calorimetry (DSC) and thermogravimetry (TG).

EXPERIMENTAL

Preparation of compounds

The ligands *dl*-2,3-butanediamine (*dl*-bn) and their complexes $[Ni(H_2O)_2(dl\text{-}bn)_2]X_2$ (X is Cl^- or Br^-), were obtained using methods described in the literature [8]. Their chemical formulae were determined by elemental analysis, and were consistent with IR spectral and magnetic measurements [3].

Apparatus

Thermogravimetry (TG) and differential thermal analysis (DTA) were performed with a Rigaku Thermoflex TG-DTA MJ800PF2 apparatus. DSC measurement was made with a Shinku-Riko DSC-1500 M5/L [7, 9–11]. The output voltages of the DSC were amplified by a Unipulse U350A and the data were acquired on a microcomputer (Epson QC10 II) via an AD converter (Thinky SC-51). The DSC measurements were performed at heating rates of 2.3, 3.4, 4.6, and 6.9 K min^{-1} and α-alumina was used as reference material. The energy output of the DSC was calibrated from the heat of dehydration of potassium nitrate ($\Delta H = 5.4$ kJ mol^{-1} at 400.9 K) and fusion of indium (99.999%) ($\Delta H = 3.3$ kJ mol^{-1} at 430 K) [12].

In each measurement, about 3–4 mg of the powdered specimens were weighed into aluminum crucibles and about 1000 data points were collected at regular intervals of time over the transitions.

X-ray diffraction patterns of powder specimens were taken with nickel-filtered Cu Kα radiation on a Rigaku Rado-C diffractometer.

Infrared spectra were measured from 250 to 4000 cm^{-1} in Nujol with a Hitachi 295 spectrophotometer.

Electronic spectra of the visible region were measured on solids with a Hitachi U-3200 spectrophotometer equipped with a head-on photomultiplier (150-0903). Spectra at elevated temperatures were obtained using a heating block [7].

Kinetic analysis

The kinetics of the thermal reaction of these complexes was studied on the basis of the DSC curves. The rate of a solid-state reaction is expressed by

$$\mathrm{d}\alpha/\mathrm{d}t = kF(\alpha) \tag{1}$$

where α is the fraction of reaction after time t, $F(\alpha)$ is a function depending on the reaction mechanism [13–15] and k is a rate constant which is related to absolute temperature T according to the Arrhenius equation

$$k = A\ \exp(-E/RT) \tag{2}$$

where A, E and R are the pre-exponential factor, the activation energy and the gas constant, respectively. Substituting eqn. (2) into eqn. (1) and assuming a linear heating rate $\beta = \mathrm{d}T/\mathrm{d}t$,

$$[(\mathrm{d}\alpha/\mathrm{d}T)\beta] = A\ \exp(-E/RT)F(\alpha) \tag{3}$$

and the logarithmic form of eqn. (3).

$$\ln[(\mathrm{d}\alpha/\mathrm{d}T)\beta] - \ln F(\alpha) = \ln A - E/RT \tag{4}$$

In the present study, the rate of reaction $[(\mathrm{d}\alpha/\mathrm{d}T)\beta]$ was directly determined from the DSC measurements. The suitability of the $F(\alpha)$ selected for the reaction was judged from the linearity of the plots of the left-hand side against $1/T$, in accordance with eqn. (4) (Achar's plot) [16].

The activation energy was determined from the slope. The activation energy obtained was checked by the modified Friedman method described previously [10, 17]. In order to determine the value of A, the experimental values of $[(\mathrm{d}\alpha/\mathrm{d}T)\beta]$, E and $F(\alpha)$ were introduced into eqn. (4).

The fraction of reaction α at a temperature T_I was derived from the ratio of the area corresponding to the heat evolved up to T_I to the integral area for the heat of the total reaction [7].

RESULTS AND DISCUSSION

It has been reported [2–4] that the complexes of *trans*-$[\mathrm{Ni(H_2O)_2}(dl\text{-}\mathrm{bn})_2]\mathrm{Cl_2}$ and *trans*-$[\mathrm{Ni(H_2O)_2}(dl\text{-}\mathrm{bn})_2]\mathrm{Br_2}$ are dehydrated at temperatures ranging from 70 to 90°C. These dehydrations are accompanied by thermochromism from violet to yellow

$$trans\text{-}[\mathrm{Ni(H_2O)_2}(dl\text{-}\mathrm{bn})_2]\mathrm{Cl_2} \rightarrow [\mathrm{Ni}(dl\text{-}\mathrm{bn})_2]\mathrm{Cl_2} + 2\mathrm{H_2O} \tag{a}$$

$$trans\text{-}[\mathrm{Ni(H_2O)_2}(dl\text{-}\mathrm{bn})_2]\mathrm{Br_2} \rightarrow [\mathrm{Ni}(dl\text{-}\mathrm{bn})_2]\mathrm{Br_2} + 2\mathrm{H_2O} \tag{b}$$

In addition, the dehydrated complexes isomerize from a square-planar (Sp) to an octahedral structure (Oh) at temperatures ranging from 180 to 190°C.

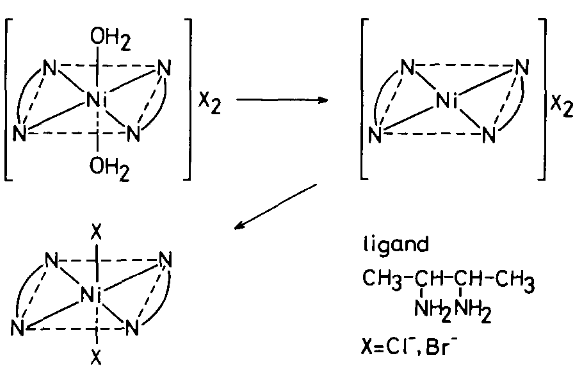

Fig. 1. Schematic expression of the isomerizations of the complexes.

$[Ni(dl\text{-}bn)_2]Cl_2$ (Sp) → *trans*-$[NiCl_2(dl\text{-}bn)_2]$ (Oh) (c)

$[Ni(dl\text{-}bn)_2]Br_2$ (Sp) → *trans*-$[NiBr_2(dl\text{-}bn)_2]$ (Oh) (d)

The dehydrations (a) and (b), and the isomerizations (c) and (d) are structural transformations, as shown schematically in Fig. 1.

Figure 2 shows the DSC and the TG curves obtained for these complexes. In the DSC curves, two endothermic peaks are observed at 84 and 73°C corresponding to the dehydrations (a) and (b), respectively. After dehydration, endothermic peaks due to the isomerizations (c) and (d) are observed, without any weight change, at temperatures ranging from 180 to 190°C. In addition, before and after the endothermic reactions (c) and (d), the colors of the specimens changed distinctly from yellow to violet and blue-violet, respectively. The colors changed reversibly and slowly from violet (or blue-violet) to yellow on cooling the specimens to room temperature.

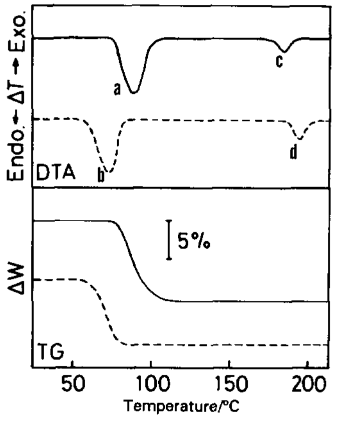

Fig. 2. DSC and TG curves of (——) $[Ni(H_2O)_2(dl\text{-}bn)_2]Cl_2$ and (– – –) $[Ni(H_2O)_2(dl\text{-}bn)_2]Br_2$; peaks a and b, and peaks c and d, correspond to the dehydrations and isomerizations, respectively (see text).

TABLE 1

$F(\alpha)$ function, activation energy E, pre-exponential factor A and enthalpy change ΔH for the dehydrations (a) and (b), and for the isomerizations (c) and (d)

Reaction	$F(\alpha)$ [a]	E/kJ mol^{-1}	$\log(A/\mathrm{s})$	ΔH/kJ mol^{-1}
(a)	$A_{1.6} \rightarrow F_1$	80.1 ± 5.6	9.6	113.6 ± 6.5
(b)	A_2	87.5 ± 3.8	11.2	102.5 ± 4.7
(c)	$A_2 \rightarrow F_1$	405.4 ± 36.4	44.0	11.4 ± 0.87
(d)	$A_{1.8} \rightarrow F_1$	223.8 ± 30.9	23.4	12.9 ± 1.6

[a] $A_n = (1-\alpha)[-\ln(1-\alpha)^{(n-1)/n}]$. $F_1 = -\ln(1-\alpha)$.

The values of the enthalpy changes ΔH for the dehydrations and the isomerizations are shown in Table 1. There is little difference in the values of ΔH between the dehydrations (a) and (b), and the isomerizations (c) and (d). These enthalpy changes are attributed to many stages, including the bond cleavage and formation, and to other factors such as changes in lattice energy, steric repulsion, etc. Detailed analysis of the ΔH values cannot be given at present because the crystal structures of these complexes before and after isomerization have not been determined.

Figure 3 shows Achar's plot for dehydration (b) in accordance with eqn. (4). In the present study, we examined plots for the nine models of $F(\alpha)$ [11]. Plots of the F_1, A_2, and R_2 mechanisms show the best linearity over nearly the whole range of reaction. The values of the activation energies E from these plots are listed in Table 2 together with their correlation coefficients. In order to select the most reliable function from these three functions, the values of E were compared with that obtained from the modified Friedman method [9, 17].

Figure 4 shows the modified Friedman plot for dehydration (b). Parallel lines are apparent in the range $0.10 < \alpha < 0.90$. The mean value of E determined from the slopes of these lines was 87.5 ± 3.8 kJ mol^{-1}. This

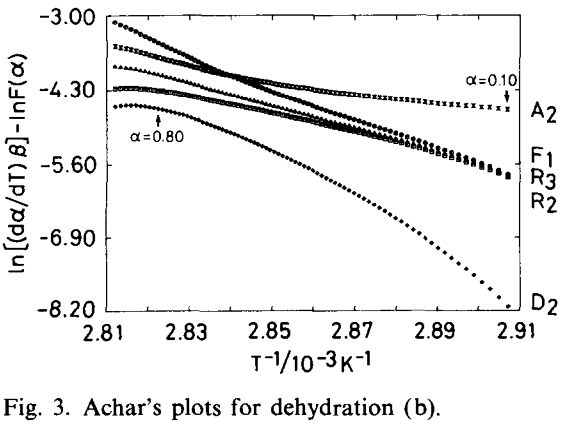

Fig. 3. Achar's plots for dehydration (b).

TABLE 2

Estimation of $F(\alpha)$ and activation energy E for the dehydration (b) using Achar's method [a]

$F(\alpha)$	α range	E/kJ mol^{-1}	r [b]
R_2	0.10–0.80	144.5	0.9972
F_1	0.10–0.80	216.4	0.9923
A_2	0.10–0.80	86.8	0.9987

[a] Results from the data obtained at a heating rate of 4.6 K min^{-1}. [b] Correlation coefficient.

value compares well with that of 86.8 kJ mol^{-1} obtained from Achar's plot for the A_2 function. Therefore, we suggest that the A_2 function is a reasonable model for dehydration (b).

The $F(\alpha)$ model for dehydration (a) was also determined as an expression of $A_{1.6}$ ($A_{1.6} = (1-\alpha)[-\ln(1-\alpha)]^{(1-1/1.6)}$). However, the function seems to change from $A_{1.6}$ to F_1 ($F_1 = [-\ln(1-\alpha)]$) in the range $0.6 < \alpha < 0.90$ (Fig. 5). The A_n model, where $A_n = (1-\alpha)[-\ln(1-\alpha)]^{(n-1)/n}$ and $1 < n < 2$, is to be the kinetic expression concerned with random nucleation and nuclei growth processes. Hulbert [18] has demonstrated the relationship between the growth of nuclei and diffusion processes as follows: when (i) the nucleation rate is assumed to be constant, (ii) the nuclei growth two-dimensionally, and (iii) the growth is controlled by the diffusion of migrating species, then the A_n expression can be derived. However, the F_1 expression can be derived when the nucleation is instantaneously complete, and the nuclei grow according to conditions (ii) and (iii). Therefore, the above change of the $F(\alpha)$ of dehydration (a) can be interpreted as follows. The dehydration may be described by an $A_{1.6}$ function until all the nuclei are formed, but once they are formed the dehydration takes place according as an F_1 function.

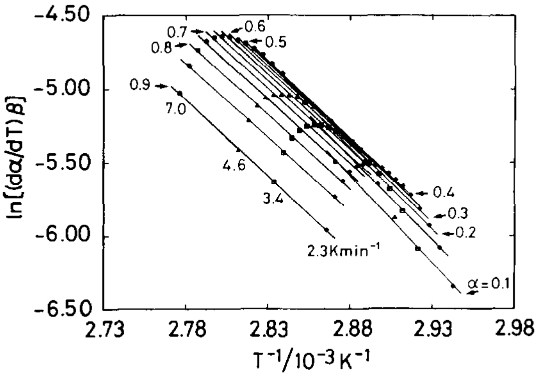

Fig. 4. Plots of $\ln[(d\alpha/dT)\beta]$ vs. $1/T$ from $\alpha = 0.10$ to 0.90 for dehydration (b).

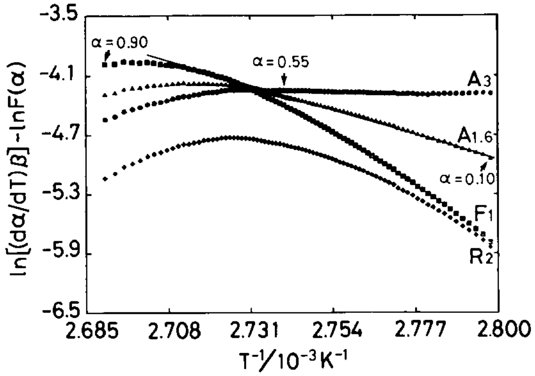

Fig. 5. Achar's plots for dehydration (a).

The isomerizations (c) and (d) were also analyzed kinetically by a similar procedure. Both reactions proceed as A_2. However, the function changes to F_1 when $\alpha > 0.9$ for (c) and $\alpha > 0.3$ for (d) (Table 2). These findings are similar to those for dehydration (a). It is worth noting that the *E* value for isomerization (c) is appreciably higher than that for (d).

For isomerization in the solid phase, the process involving anation would require that the anions leave lattice sites and migrate to the complex cation to form a transition state [7, 19]. The activation energy observed would correspond to the sum of those for both stages. The activation energy required for the initial stage is expected to increase with increasing lattice energy.

Because for a given cation, e.g. $[\mathrm{Ni}(dl\text{-bn})_2]^{2+}$, the lattice energy is assumed to increase with a decrease in anion size, it is reasonable that the crystal of the chloride complex should have a higher lattice energy than that of the bromide complex. However, the smaller counter anion may more readily migrate to the complex cation [20].

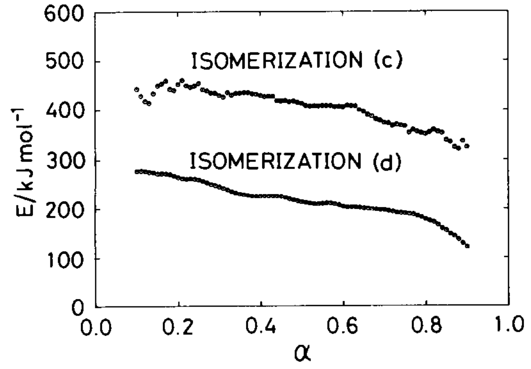

Fig. 6. Relation between activation energy *E* and fraction of isomerization α.

Figure 6 shows the relation between the activation energy determined from the modified Friedman method and the fraction of isomerization α. It is noteworthy that the values of E for the initial stages of isomerizations (c) and (d) are slightly higher than those for the later stages. This finding may be explained by way of the assumption above that an anation in solid state involves at least two stages, i.e. the migration of the counter anion from a lattice site to the complex cation and the formation of a transition state. The rate-determining steps for both the isomerizations (c) and (d) seem to be their initial steps.

Therefore, it is to be expected that the value of E for isomerization (c) is higher than that of (d). However, no simple reason can be suggested to explain why the E value for (c) is considerably higher than that for (d) because the crystal structures of these complexes before and after isomerization have not been clarified.

REFERENCES

1 R. Tsuchiya, S. Joba, A. Uehara and E. Kyuno, Bull. Chem. Soc. Jpn., 46 (1973) 1454.
2 Y. Ihara, E. Izumi, A. Uehara, R. Tsuchiya, S. Nakahara and E. Kyuno, Bull. Chem. Soc. Jpn., 55 (1982) 1028.
3 Y. Ihara, T. Kamishima and R. Tsuchiya, Thermochim. Acta, 67 (1983) 23.
4 Y. Ihara, A. Wada, Y. Fukuda and K. Sone, Bull. Chem. Soc. Jpn., 59 (1986) 2309.
5 Y. Ihara, Y. Fukuda and K. Sone, Inorg. Chem., 26 (1987) 3745.
6 Y. Ihara, Dr. Sci. Thesis, Kyushu University, Fukuoka, Japan, 1987.
7 Y. Masuda, T. Matsuda, H. Kume and Y. Ihara, Thermochim. Acta, 156 (1989) 137.
8 F.H. Dickey, W. Fikett and H.J. Lucas, J. Am. Chem. Soc., 74 (1952) 944.
9 Y. Masuda, Y. Ito, R. Ito and K. Iwata, Thermochim. Acta, 99 (1986) 205.
10 Y. Masuda, Y. Ito, R. Ito and K. Iwata, Thermochim. Acta, 102 (1986) 263.
11 Y. Masuda, K. Iwata, R. Ito and Y. Ito, J. Phys. Chem., 91 (1987) 6543.
12 The Chemical Society of Japan (Ed.), Kagaku Binran Kisohen II (Handbook of Chemistry), 3rd edn., Maruzen, Tokyo, 1984, p. 270.
13 J.H. Sharp, G.W. Brindley and B.N.N. Achar, J. Am. Ceram. Soc., 49 (1966) 379.
14 J. Šesták and G. Berggren, Thermochim. Acta, 3 (1971) 1.
15 K. Heide, W. Höland, H. Gölker, K. Seyfarth, B. Müller and R. Sauer, Thermochim. Acta, 13 (1975) 365.
16 B.N.N. Achar, G.W. Brindley and J.H. Sharp, Proc. Int. Clay Conf., Jerusalem, 1 (1966) 67.
17 H.L. Friedman, J. Polym. Sci. Polym. Chem. Ed., 6 (1964) 183.
18 S.F. Hulbert, J. Brt. Ceram. Soc., 6 (1969) 11.
19 T. Fujiwara and J.C. Bailar, Jr., Bull. Chem. Soc. Jpn., 61 (1988) 857.
20 F. Beniere and V. Hari-Babu, Cryst. Lattice Defects Amorph. Mater., 15 (1987) 263.